(2)

AD-A237 462

1991

DOCUMENTATION PAGE

Form Approved OMB No 0704 01HR

1b RESTRICTIVE MARKINGS

3 DISTRIBUTION/AVAILABILITY OF REPORT
Approved for public release and sale; its distribution is unlimited.

2b DECLASSIFICATION/DOWNGRADING SCHEDULE

4 PERFORMING ORGANIZATION REPORT NUMBER(S)
Technical Report No. 101

5 MONITORING ORGANIZATION REPORT NUMBER(S)

6a NAME OF PERFORMING ORGANIZATION
Purdue University
Department of Chemistry

6b OFFICE SYMBOL (If applicable)

7a NAME OF MONITORING ORGANIZATION
Division of Sponsored Programs
Purdue Research Foundation

6c ADDRESS (City, State, and ZIP Code)
Purdue University
Department of Chemistry
West Lafayette, IN 47907

7b ADDRESS (City, State, and ZIP Code)
Purdue University
West Lafayette, IN 47907

8a NAME OF FUNDING/SPONSORING ORGANIZATION
Office of Naval Research

8b OFFICE SYMBOL (If applicable)

9 PROCUREMENT INSTRUMENT IDENTIFICATION NUMBER
Contract No. N00014-91-J-1409

8c ADDRESS (City, State, and ZIP Code)
800 N. Quincy Street
Arlington, VA 22217

10 SOURCE OF FUNDING NUMBERS

PROGRAM ELEMENT NO	PROJECT NO	TASK NO	WORK UNIT ACCESSION NO

11 TITLE (Include Security Classification)
Solvent Dynamical Effects in Electron Transfer: The Solvent Inertial Limit and the Predicted Influence of Quantum Effects

12 PERSONAL AUTHOR(S)
G.E. McManis, A. Gochev, and M.J. Weaver

13a TYPE OF REPORT	13b TIME COVERED	14 DATE OF REPORT (Year, Month, Day)	15 PAGE COUNT
Technical	FROM _____ TO _____	May 31, 1991	

16 SUPPLEMENTARY NOTATION

17 COSATI CODES			18 SUBJECT TERMS (Continue on reverse if necessary and identify by block number)
FIELD	GROUP	SUB-GROUP	analytical continuum formulations for the solvent inertial frequency, nuclear tunneling, rate-solvent friction

19 ABSTRACT (Continue on reverse if necessary and identify by block number)

Analytical continuum formulations for the solvent inertial frequency, constituting the anticipated zero-friction limit for adiabatic barrier crossing in solvent-controlled electron-transfer processes, are derived and discussed. The role of solvent inertia in solvent dynamical effects is discussed with emphasis on the likely modifications brought about by nuclear tunneling. Approximate formulations suitable for assessing the latter correction in the presence as well as absence of solvent friction are outlined and compared. Numerical calculations are provided that illustrate the partly compensatory influence on the rate-solvent friction dependence resulting from nuclear tunneling together with reaction nonadiabaticity. Such combined quantum effects are anticipated typically to mask the clearcut emergence of solvent inertial effects on electron-transfer reaction dynamics in common low-friction media.

20 DISTRIBUTION/AVAILABILITY OF ABSTRACT
☐ UNCLASSIFIED/UNLIMITED ☐ SAME AS RPT. ☐ DTIC USERS

21 ABSTRACT SECURITY CLASSIFICATION

22a NAME OF RESPONSIBLE INDIVIDUAL

22b TELEPHONE (Include Area Code)

22c OFFICE SYMBOL

DD Form 1473, JUN 86 Previous editions are obsolete. SECURITY CLASSIFICATION OF THIS PAGE

OFFICE OF NAVAL RESEARCH

Contract No. N00014-91-J-1409

Technical Report No. 101

Solvent Dynamical Effects in Electron Transfer: The Solvent Inertial Limit and the Predicted Influence of Quantum Effects

by

G.E. McManis, A. Gochev, and M.J. Weaver

Prepared for Publication

in

Chemical Physics

Purdue University

Department of Chemistry

West Lafayette, Indiana 47907

May 1991

Solvent Dynamical Effects in Electron Transfer: The Solvent Inertial Limit and the Predicted Influence of Quantum Effects[‡]

George E. McManis, Alexander Gochev,

and Michael J. Weaver

Department of Chemistry, Purdue University

West Lafayette, Indiana 47907 (USA)

Chemical Physics

(Special Issue: "Friction in Liquid-Phase Reactions")

Submitted May 30, 1990

Revised October 15, 1990

[‡]Abstracted in part from Ph.D. thesis of G. E. McManis, Purdue University, 1989

ABSTRACT

Analytical continuum formulations for the solvent inertial frequency, constituting the anticipated zero-friction limit for adiabatic barrier crossing in solvent-controlled electron-transfer processes, are derived and discussed. The role of solvent inertia in solvent dynamical effects is discussed with emphasis on the likely modifications brought about by nuclear tunneling. Approximate formulations suitable for assessing the latter correction in the presence as well as absence of solvent friction are outlined and compared. Numerical calculations are provided that illustrate the partly compensatory influence on the rate-solvent friction dependence resulting from nuclear tunneling together with reaction nonadiabaticity. Such combined quantum effects are anticipated typically to mask the clearcut emergence of solvent inertial effects on electron-transfer reaction dynamics in common low-friction media.

I. INTRODUCTION

The realization that the dynamical properties of the solvent can play an important role in the kinetics of electron transfer, as in other condensed-phase chemical processes, has spawned an impressive range of recent studies of both an experimental and theoretical nature (see refs. 1 and 2 for recent overviews). Inquiries of the former type have encompassed examinations of activated electron-transfer (ET) reactions (i.e. featuring significant free-energy barriers),[1] as well as real-time dynamics of polar solvation as studied by ultrafast laser techniques, especially time-dependent fluorescence Stokes shift (TDFS) measurements.[2,3] These considerations have led to the conclusion that in many solvents, at least for near-ambient conditions, the nuclear reaction dynamics are determined primarily by overdamped solvent relaxation as characterized in the simplest case by the longitudinal relaxation time, τ_L. In other words, the common occurrence of solvent friction depresses the net frequency of adiabatic barrier crossing below the value, $\omega_o/2\pi$ (s^{-1}), reflecting the inertia of individual solvent dipoles. The latter frequency is that expected on the basis of transition-state theory (TST) treatments.

Nevertheless, it is anticipated that in some circumstances the solvent friction will be sufficiently small so that $\tau_L^{-1} \geq \omega_o$, whereupon the rate of barrier crossing can be determined partly or wholly by the longitudinal *inertial* polarization dynamics as reflected in ω_o, rather than by the over-damped frequency τ_L^{-1}. In principle, inertial-limiting effects could be discerned by non-exponential TDFS decays at short times[4] and also from τ_L-independent barrier-crossing frequencies for suitably adiabatic ET processes.[5] In contrast to overdamped motion, however, no clearcut experimental observation of such inertial effects in polar solvents has apparently been reported. Such observations are hampered by the high frequencies anticipated for solvent dipole inertia, typically $\omega_o \geq 5 \times 10^{12}$ s^{-1} for typical dipolar solvents. Since thereby $\omega_o \geq k_B T/\hbar$ (where k_B is the Boltzmann constant) at

ambient temperatures, quantum effects may commonly be anticipated, specifically involving nuclear tunneling so to enhance the barrier-crossing rate above the expectations of classical dynamics. An additional major limitation to the emergence of solvent inertial effects is that the maintenance of reaction adiabaticity, whereupon the full effect of nuclear dynamics upon the ET rates will be felt even at such rapid frequencies, requires large degrees of donor-acceptor electronic coupling.[6,7] Conversely, diminishing values of the electronic transmission coefficient, κ_{el}, are often expected as the friction is decreased by altering the solvent,[6] so that such reaction nonadiabaticity can often curtail the influence of solvent inertia on the barrier-crossing dynamics under these conditions. Consequently, then, the occurrence of inertial limiting effects on solvent-dependent ET reaction rates may be obscured by the increasingly accelerating and retarding influences of nuclear tunneling and reaction nonadiabaticity, respectively, as the nuclear dynamics become more facile.

The central issue addressed herein is the numerical assessment of the likely role and importance of solvent inertia on ET reaction rates given the inevitable additional presence of such quantum effects. The organization of the paper is as follows. We first discuss specific analytic formulations for the inertial limiting frequency and related quantities, so to characterize the magnitudes and physical origins of such effects, and to provide approximate estimates of ω_o. The latter is of practical interest given the absence of direct experimental information on inertial frequencies. We then outline theoretical formulations that enable the nuclear quantum corrections to be made in the presence as well as absence of solvent friction. This is followed by representative numerical calculations so to illustrate the likely experimental consequences of coupled inertial-quantal effects upon ET exchange rates in low-friction media. Of particular interest here is the manner in which these factors are liable to influence rate-solvent friction dependencies

since this issue is of specific relevance to recent (and ongoing) experimental studies.[6,7] While the emphasis here is on the practical consequences of such effects, some explanative discussion of the underlying physical origins is provided since we found the theoretical literature on this topic often to be as esoteric as it is extensive.

II. SOLVENT INERTIAL EFFECTS ON THE ELECTRON-TRANSFER RATE CONSTANT

1. Inertial Limiting Frequency

The unimolecular rate constant for an electron-transfer reaction (such as within a given internuclear reactant geometry for a bimolecular outer-sphere reaction[7]) is conveniently expressed as[8]

$$k_{et} = \Gamma_n \kappa_{el} \nu_n \exp(\Delta G^*/k_B T) \tag{1a}$$

$$= \Gamma_n \kappa_{el} k_A \tag{1b}$$

where ν_n is the nuclear frequency factor and ΔG^* is the activation free energy. The terms Γ_n and κ_{el} provide quantum corrections to the "classical" adiabatic rate constant k_A arising from nuclear tunneling and electronic nonadiabaticity, respectively. For a given reaction, most simply for a fixed ΔG^* and for a given donor-acceptor electronic coupling (as gauged by the electronic matrix coupling element H_{12}), Γ_n will tend to increase and κ_{el} to decrease for progressively larger ν_n values as engendered most readily by altering the solvent. For suitably small ν_n, on the other hand, both Γ_n and κ_{el} approach unity so that $k_{et} \simeq k_A$.

In high-friction ("overdamped") solvents, the adiabatic barrier-crossing frequency ν_n is characterized in the continuum limit by τ_L^{-1}, this frequency can fall substantially below the TST-limit value, $\omega_o/2\pi$. Nevertheless, theoretical treatments suggest that ν_n is not greatly different from $\omega_o/2\pi$ in some media, so that significant solvent inertial effects on the reaction dynamics might often be anticipated. Especially since direct experimental information on solvent inertial frequencies are lacking, at least approximately reliable analytic formulations of ω_o are clearly desirable. We now

consider specific expressions for ω_o, along with their physical basis.

A straightforward formulation of ω_o has been given by Hynes, who wrote (but without derivation) the following expression[9]

$$\omega_o^2 = \frac{(2\epsilon_s + \epsilon_\infty)\ \omega_f^2}{3\epsilon_\infty\ g_K} \tag{2}$$

In Eq. (2), ϵ_s and ϵ_∞ are the static and "infinite" frequency dielectric constants, and ω_f is the "free rotor" frequency which for linear and spherical-top molecules is given by

$$\omega_f^2 = 2k_B T/I \tag{2a}$$

where I is the moment of inertia. In Appendix A, we present a complete derivation of Eq. (2).

The presence of the Kirkwood "g" factor in Eq. (2), g_K, indicates that solvent structural factors are important in determining ω_o. The Kirkwood-Frolich formula is an adequate means of calculating g_K in this context[10]:

$$g_K = \frac{9k_B T\ (\epsilon_s - \epsilon_\infty)(2\epsilon_s + \epsilon_\infty)}{4\pi N\mu_v^2 \qquad \epsilon_s(\epsilon_\infty + 2)^2} \tag{3}$$

where N is the Avogadro Number and μ_v is the gas-phase dipole moment.

Equation (2) reduces to an expression given earlier by Calef and Wolynes[5] for polar, non-polarizable media by setting $g_K = 1$ and $\epsilon_\infty = 1$ for the special case of a rigid rotor. Their equation (72) in our nomenclature reads:*

---

* Several misprints in ref. 5 should be noted in this connection. Equation 73 in ref. 5 should read (in their notation):

$$r = \frac{1}{2\pi}\ \left(\frac{k}{m}\right)^{1/2} \exp(-\beta\Delta F^{\ddagger})$$

Equation 77 should read:

$$r = \frac{\tau_{ROT}^{-1}}{2\pi}\ (2\epsilon_s\ \gamma)^{1/2} \exp(-\beta\Delta F^{\ddagger})$$

and the equation for k in Table I should read:

$$k = \frac{1}{\tau_L}\left[\frac{1}{2} + \frac{1}{2}\left[1 + \frac{2\tau_R^2}{\tau_L^2\ \epsilon_s\ C^2\ \gamma}\right]^{1/2}\right]^{-1}\ \frac{\exp(-\beta\Delta F^{\ddagger})}{2\pi C}$$

$$\omega_o = \left(\frac{k_B T}{I}\right) \left(\frac{6y\ \epsilon_s}{\epsilon_s - 1}\right)^{1/2} \tag{4}$$

where y, the reduced concentration of dipoles is given by[11]

$$y = \frac{4\pi\ \rho\mu^2\beta}{9} \tag{4a}$$

where ρ is the solvent density. Equation (4) can be rearranged to yield a formula having the same structure as Eq. (2):

$$\omega_o^2 = \left(\frac{2k_B T}{I}\right) \left(\frac{(2\epsilon_s + 1)}{3g_K}\right) \tag{5}$$

Equation (5) can also be expressed in the following form:[5]

$$\omega_o = \left[\left(\frac{2k_B T}{I}\right) \epsilon_s\ \gamma\right]^{1/2} \tag{6}$$

where

$$\gamma = \frac{\epsilon_s - 1}{3y} = \frac{4\pi\ \rho\mu^2\beta}{3k_B T(\epsilon_s - 1)} = \frac{1}{1 + \frac{\rho}{\Omega} h_o} \tag{6a}$$

and Ω is a normalizing volume element and h_o is the pair correlation function.[12] This formulation reemphasizes how the solvent structure (via γ) influences ω_o and hence the TST reaction rate. The use of Eq. (5) typically yields ca twofold lower estimates of ω_o compared with Eq. (2) owing to the neglect of ϵ_∞ in the former.

It is interesting to note that the expression for ω_o given in Eq. 2 is also similar to that for the "dipolaron frequency" identified by Madden and Kivelson.[13] These authors developed a "three variable theory" to describe the complex, frequency-dependent dielectric constant, $\epsilon(\omega)$. The variables, Ω_R, Ω_T and Γ are used to characterize three distinctly different processes that occur in dipolar fluids. Two variables, Ω_R and Ω_T, describe dipolar rotational and librational frequencies, respectively; the last variable, Γ, describes how Ω_R and Ω_T are damped. All three of these quantities are con-

sidered in the context of a time correlation function, $\Phi(t)$, which is related to $\hat{\epsilon}(\omega)$ using the one-sided Fourier-Laplace transform, $\mathcal{L}_{i\omega}$:

$$\hat{\epsilon}(\omega) = \epsilon_\infty + (\epsilon_s - \epsilon_\infty)\ [1 + \mathcal{L}_{i\omega}\ (\Phi(t))] \tag{7}$$

Although all three variables combine to dictate the polarization dynamics through $\hat{\epsilon}(\omega)$, Ω_R is most relevant to this discussion. This quantity represents an inertial frequency (that is, a frequency which is inversely proportional to the moment of inertia) that characterizes collective dipolar motions contained in the short-time behavior of $\Phi(t)$. For linear and spherical top molecules:

$$\Omega_R^2 = \frac{(2\epsilon_s + \epsilon_\infty)}{3\epsilon_s g_k} \cdot \frac{2k_B T}{I} \tag{8}$$

The dipolaron frequency is the longitudinal counterpart of Ω_R:

$$\omega_o^2 = \Omega_R^2(\epsilon_s/\epsilon_\infty) \tag{9}$$

as can be seen by comparing Eqs. (8) and (9) with Eq. (2) (see Appendix A).

Poley originally predicted the presence of a spectral feature on the basis of the differences between ϵ_∞ and the square of the refractive index at infrared frequencies for "Debye" fluids such as nitrobenzene.[14] He noted that this difference was proportional to μ^2 and considered this unambiguous evidence for a dielectric loss associated with molecular reorientation. This "Poley" absorbance has since been observed in most polar liquids that have been studied in the far infrared region.[15] Unfortunately, ω_o cannot be related directly to the frequency of the Poley band: the absorbance is associated with the librational reorientation of solvent dipoles in the "cage" formed by neighboring molecules, which is a transverse (Ω_T), not a longitudinal, oscillation.[13] The Poley band is noted here since it constitutes one of several high frequency dipole reorientations that have yet to be considered in the context of their relevance (or lack thereof) for electron-

transfer processes.

The practical applicability of Eq. (2) is subject to several important constraints. One underlying assumption, of course, is the dielectric-continuum approximation. Although the presence of molecular moments of inertia and dipole moments in Eq. (2) implies some innate consideration of solvent molecularity, the many countervailing assumptions that are made to assure tractability may lead to some serious uncertainties in the numerical predictions.[17] Nonetheless, one can use Eq. (2) as well as molecular-dynamics simulations to provide reasonable estimates of ω_o.

Estimates of ω_o obtained from Eq. (2) for some common polar solvents, encompassing a typical range of dynamical properties (at 25°C), are listed in Table I alongside corresponding values of τ_L^{-1}. The first five solvents each exhibit roughly Debye behavior (i.e. exhibit only a single clearcut dispersion in the dielectric loss spectrum). While the τ_L^{-1} values for these solvents vary by up to ca 40 fold, the inertial frequencies are seen to vary to a markedly smaller extent. Given that with the exception of acetonitrile, $\tau_L^{-1} << \omega_o$, one might expect that solvent inertial effects upon electron-transfer dynamics may commonly be unimportant at ambient temperatures. However, acetonitrile is but one member of a class of low-friction solvents (also acetone, nitromethane, etc.), for which inertial effects may well play a significant role.

Corresponding molecular dynamics simulations of ω_o are as yet uncommon. Nevertheless, such calculations yield, for example, values of 95 ps^{-1} for water[19] and 23.5 ps^{-1} for acetonitrile.[20] These values are within ca twofold of (albeit slightly higher than) the corresponding estimates in Table I. Given the uncertainties contained in both Eq. (2) and the simulations, this agreement is acceptable.

For larger solvent molecules, however, molecular asymmetry and breakdown of dielectric continuum theory may prove a more serious limitation to

the applicability of Eq. (2). Furthermore, the use of Eq. (2) together with a friction kernel for the rate expression that does not include the short time dynamics of the longitudinal polarization modes brings a logical inconsistency into the calculations.[18] The complex nature of these high-frequency processes has been described in detail.[16,21] Further insight into dielectric relaxation processes that can be gleaned from inertial effects is detailed in Appendix B of ref. 30. For the calculations that follow, we choose $\omega_o/2\pi$ values over the range 5 to 25 ps^{-1}, reflecting the anticipated range for typical solvents (Table I).

2. Classical Adiabatic Rate Expressions

In the absence of solvent friction (i.e. in the TST limit) the classical adiabatic barrier-crossing frequency, ν_n, (i.e. when $\Gamma_n = 1$, $\kappa_{el} = 1$) will equal $\omega_o/2\pi$ irrespective of the shape of the barrier top as influenced by the electronic coupling matrix element, H_{12}. In the presence of solvent friction, however, ν_n should generally be sensitive to the barrier-top curvature.[18] Although such treatments for electron-transfer reactions have been discussed previously,[9,18] the relevant relationships and the underlying physics are now summarized briefly since they are utilized in the ensuing numerical calculations.

In general, the friction at the barrier top is probed at different crossing frequencies than the function experienced by a particle climbing up (or sliding down) the well. It is useful to make a piecemeal parabolic approximation to the true potential-energy surface: fitting two parabolae to the wells and an inverted parabola to the barrier top.[9] Since ω_o is the characteristic frequency of oscillations in the wells, simple algebraic arguments yield an equivalent frequency near the barrier top given by[18]

$$\omega_b = \omega_o \left(\frac{2\Delta G_c^*}{H_{12}} - 1\right)^{1/2} \qquad (10)$$

where ΔG_c^* is the "cusp" barrier height, i.e. in the limit where $H_{12} \to 0$. One may then consider the overall adiabatic rate constant k_A as a composite of the rate for crossing the barrier top, k_b, and that for diffusion in the wells, k_w:

$$k_A^{-1} = k_b^{-1} + 0.5\ k_w^{-1} \tag{11}$$

Equation (11) is a restatement of the Northrup-Hynes "Stable States Picture" of barrier crossing dynamics, applicable if $\Delta G^* \gtrsim 2\text{-}3\ k_B T$.[9,22]

An expression for k_b in the classical limit is the Grote-Hynes formula:[9,22,23]

$$k_b = \frac{\lambda_R}{2\pi}\ \frac{\omega_o}{\omega_b}\quad \exp(-\Delta G^*/k_B T) \tag{12}$$

where λ_R is a reactive (or, equivalently, memory renormalized) frequency that corresponds to the largest positive root of the equation

$$\lambda_R = \frac{\omega_b^2}{\lambda_R + \eta(\lambda_R)} \tag{12a}$$

given the frequency-dependent friction, $\eta(\lambda_R)$. For simplicity, the calculations here consider only Debye solvents, so that the friction is frequency independent and $\eta = \omega_o^2\ \tau_L$.[18]

The treatment of k_w requires a different approach. Hynes derived an integral expression for the temporal characteristics of a Gaussian (but not necessarily Markov) process leading to k_w.[9] In the Debye limit this simplifies approximately to[5,9]

$$k_w = 2\tau_L^{-1}\ \left(\frac{\Delta G_c^*}{4\pi k_B T}\right)^{1/2} \exp(-\Delta G^*/k_B T) \tag{13}$$

In the limiting case where $\tau_L = 0$, $\eta = 0$, the ratio of λ_r/ω_b appearing in Eq. (17) is unity. As then $k_w >> k_b$, the resulting expression for k_A is the usual TST result:

$$k_A \approx k_b \approx (\omega_o/2\pi)\ \exp(-\Delta G^*/k_B T) \tag{14}$$

More generally, in the presence of friction k_A can be obtained from Eqs. (11)-(13), which also enables the classical adiabatic barrier-crossing frequency ν_n [Eq. (1)] to be found from

$$\nu_n = k_A\ \exp(\Delta G^*/k_B T) \tag{15}$$

III. QUANTUM CORRECTIONS TO THE CLASSICAL ADIABATIC RATE CONSTANT

As already noted, the influence of the nuclear and electronic quantum corrections, as contained in Γ_n and κ_{el}, upon the reaction rate will systematically be greater for larger ν_n values. Unlike ν_n itself, the magnitude of both Γ_n and κ_{el} in the absence of solvent friction is expected to be sensitive to the shape of the barrier top as well as the wells. Thus diminishing the extent of donor-acceptor electronic coupling (i.e. decreasing H_{12}) will enlarge ω_b at a given ω_o, which will enhance the extent of nuclear tunneling (i.e. increase Γ_n) as well as lessen the efficiency of electron tunneling (i.e. decrease κ_{el}). The diminution of ν_n for a given barrier shape brought about by the presence of solvent friction will tend to decrease the magnitude of these quantum corrections (i.e. depress Γ_n, enlarge κ_{el}).

Consequently, then, the manner in which such quantum corrections can influence solvent dynamical effects in electron transfer is a complex interplay between several factors. As a prologue to evaluating typical numerical consequences of such quantum effects, we now outline and evaluate some candidate analytical expressions.

1. Nuclear-Tunneling Corrections

A convenient expression for nuclear tunneling through a parabolic barrier top in the TST limit (i.e. when $\nu_n = \omega_o/2\pi$) is:[24,25]

$$\Gamma_n = \left(\frac{\omega_b}{\omega_o}\right) \frac{\sinh\ (\hbar\ \omega_o/2k_B T)}{\sin\ (\hbar\ \omega_b/2k_B T)} \tag{16}$$

At higher temperatures ($\hbar\omega_o/2k_BT \ll 1$), Eq. (16) can be approximated by[26]

$$\Gamma_n \approx \frac{(\hbar\ \omega_b/2k_BT)}{\sin\ (\hbar\ \omega_b/2k_BT)} \approx \frac{(\pi\ T_k/2T)}{\sin\ (\pi\ T_k/2T)} \qquad (17)$$

here T_k is a "characteristic temperature" of the system, such that at $T = T_k$ the probability for transitions above the barrier and those through it are equal. This latter formulation is of particular value as a diagnostic tool: if $T < \frac{1}{2}\ T_k$, large nuclear tunneling effects are predicted whereas for $T > 2T_k$ tunneling effects will be small or negligible.[26]

Both formulas given above face restrictions concerning the admissible degree of barrier curvature; specifically, they require that $\hbar\omega_b < 2\pi k_BT$ to assure that Γ_n remains a positive definite quantity. These approximate formulations also face difficulties when Γ_n is large (say, > 5-10).[27] Such a circumstance indicates that tunneling from deep within the well is significant, complicating the analysis.

An expression for the tunneling correction that is appropriate for cusp-like barriers (i.e. when H_{12} is small) has been given by Holstein:[28]

$$\Gamma_n = \left[\frac{\sinh\ (\hbar\ \omega_o/2k_BT)}{(\hbar\ \omega_o/2k_BT)}\right]^{\frac{1}{2}} \exp\left(-\left(\frac{4\Delta G_c^*}{\hbar\ \omega_o}\right)\ \left[\tanh\left(\frac{\hbar\ \omega_o}{4k_BT}\right) - \frac{\hbar\ \omega_o}{4k_BT}\right]\right) \qquad (18)$$

Equation (18) should be valid over a wide temperature range.

Introducing friction into the nuclear-tunneling correction, as is needed here, requires a rather more involved analysis. A lucid discussion of the quantum corrections to the transition state theory and the generalized quantum Kramer's theory has been provided by Hanggi.[24] As noted there, and by Wolynes,[29] the ratio of λ_R/ω_b that distinguishes the classical adiabatic rate constant k_b from k_{TST} [Eq. (12)] also serves to renormalize the characteristic temperature, T_k, used in the calculation of Γ_n [Eq. (17)]. Stated differently, by regarding λ_R as a memory renormalized frequency, the presence

of energy dissipation acts to change the path and frequency of barrier crossing.[24] In the present analysis, the nuclear-tunneling correction, $\tilde{\Gamma}_n$, is taken into account entirely in the "barrier-top" component, k_b, of the overall rate constant k_A [Eqs. (11), (12)]:

$$k_b = \tilde{\Gamma}_n \, (\lambda_R/\omega_b)(\omega_o/2\pi) \, \exp(-\Delta G^*/k_B T) \tag{19}$$

The overall nuclear-tunneling correction, Γ_n, in Eq. (1) is thereby smaller than $\tilde{\Gamma}_n$, being weighted by the relative magnitudes of k_b and k_w:

$$\Gamma_n = \frac{(2k_b + k_w)\, \tilde{\Gamma}_n}{2\tilde{\Gamma}_n \, k_b + k_w} \tag{20}$$

While this formulation satisfactorily considers the nuclear-tunneling correction to k_b, it can also be questionable if $\tilde{\Gamma}_n$ is large since a tunneling correction to k_w would also then be necessary.

A useful, albeit cumbersome, formulation of $\tilde{\Gamma}_n$ was derived by Wolynes[29] and by Daknovskii and Ovchinnikov[25] (and recapitulated lucidly by Hanggi[24]):

$$\tilde{\Gamma}_n = \frac{\Gamma(1 - \lambda^+/\theta)\, \Gamma(1 - \lambda^-/\theta)}{\Gamma(1 - \Lambda^+/\theta)\, \Gamma(1 - \Lambda^-/\theta)} \tag{21}$$

where for Debye solvents

$$\lambda^{\pm} = \frac{-\eta}{2} \pm \left(\frac{\eta^2}{4} + \omega_B^2\right)^{1/2} \tag{21a}$$

$$\Lambda^{\pm} = \frac{-\eta}{2} \pm \left(\frac{\eta^2}{4} - \omega_o^2\right)^{1/2} \tag{21b}$$

given $\theta = 2\pi k_B T/\hbar$ and $\eta = \omega_o^2 \tau_L$. The variables λ^+ and λ^- are familiar as the two poles obtained from the Grote-Hynes analysis for the case of frequency-independent friction.[9,22,23] Equation (21b) establishes the (memory renormalized) frequencies characterizing fluctuations about the minimum.

Note that Eq. (21) has simple poles at $\Lambda^+/\theta = 1$ and at $\Lambda^-/\theta = 1$. Moreover, Eq. (21b) becomes complex for $\eta < 2\omega_o$.

It can be shown that Eq. (21) reduces analytically to Eq. (16) in the zero-friction limit.[30] Given that Eq. (16) can be approximated under some conditions by Eq. (17), this suggests that Eq. (21) might also be approximated by the memory renormalized version of Eq. (17):

$$\tilde{\Gamma}_n \approx \frac{\lambda_R}{\omega_o} \frac{\sinh(\hbar\,\omega_o/2k_BT)}{\sin(\hbar\,\lambda_R/2k_BT)} \tag{22}$$

The effect of friction upon $\tilde{\Gamma}_n$ is therefore considered to arise simply from the diminution of the net velocity along the reaction coordinate close to the barrier top from the TST value, ω_b, to λ_R. This treatment of friction effects in terms of renormalized velocities is closely analogous to procedures commonly used to describe such effects upon reaction nonadiabaticity (vide infra).[7] We have found Eq. (22) to be a good approximation to Eq. (21) (within ca. 20%) over the range of parameters encountered in the numerical calculations described below. Equation (22) has the virtue of allowing the examination of the complete rate-friction regime, using a single, physically transparent, formula. Another simple expression which provides a reasonable approximation to Eq. (21) is [9](cf ref. 31):

$$\tilde{\Gamma}_n \approx \exp((\hbar/k_BT)^2(\omega_B^2 + \omega_o^2)/24) \tag{23}$$

In view of Eq. (10), Eq. (23) can be rewritten as

$$\tilde{\Gamma}_n \approx \exp((\hbar/k_BT)^2\Delta G_c^*\,\omega_o^2/12H_{12}) \tag{24}$$

Equation (24) emphasizes the sensitivity of $\tilde{\Gamma}_n$ to ω_o, H_{12} and the temperature.

Appendix B presents a brief numerical comparison of nuclear-tunneling factors extracted using some formulae presented in this section.

2. Nonadiabaticity Corrections

The anticipated influence of reaction nonadiabaticity [i.e. $\kappa_{el} < 1$ in Eq. (1)] on the ET rate-solvent friction dependence is well documented.[1,7,9,32,33] The prediction that the extent of this dependence can be sensitive to both the donor-acceptor electronic coupling and the magnitude of the friction has recently received direct experimental verification.[6] Since we have discussed the treatment of such electronic nonadiabaticity effects in detail elsewhere,[7] our remarks here are confined to a brief summary of simplified formulae relevant to the numerical calculations described below.

A generally useful expression for nonadiabatic effects upon the unimolecular ET rate constant in the presence of solvent friction is[7]

$$k_{et} = \frac{\tilde{\kappa}_{el}\, k^{TST}}{1 - \tilde{\kappa}_{el} + [\tilde{\kappa}_{el} k^{TST}/k_A]} \tag{25}$$

where k^{TST} is the rate constant corresponding to the adiabatic TST limit, and $\tilde{\kappa}_{el}$ is related to the overall electronic transmission coefficient κ_{el} by

$$\kappa_{el} = \tilde{\kappa}_{el}/[\kappa_a + \tilde{\kappa}_{el}(1 - \kappa_a)] \tag{26}$$

where $\kappa_a = k_A/k^{TST}$. The $\tilde{\kappa}_{el}$ values are related to the extent of electronic coupling by[7]

$$\tilde{\kappa}_{el} = 4\pi^{3/2}\gamma_T/(+ 4\pi^{3/2}\gamma_T) \tag{27}$$

where

$$\gamma_T = |H_{12}|^2/4\hbar\omega_o(\Delta G^* k_B T)^{1/2} \tag{27a}$$

A particularly straightforward, albeit more approximate, formulation of κ_{el} which is applicable either in the presence or absence of friction is the Landau-Zener multiple-crossings expression[7,32]

$$\kappa_{el} = \frac{2[1 - \exp(-\nu_{el}/2\nu_n)]}{2 - \exp(-\nu_{el}/2\nu_n)} \tag{28}$$

where the "electronic frequency factor" ν_{el} is given by

$$\nu_{el} = H_{12}^2 (\pi/16\Delta G^* \hbar^2 k_B T)^{1/2} \tag{28a}$$

Since the nuclear frequency factor ν_n describes the net velocity for classical adiabatic passage over the barrier top, it accounts simply for the effect of solvent friction upon κ_{el} [cf Eq. (22) for nuclear tunneling]. Equation (28) therefore provides a useful means of interpolating between the adiabatic limit (where $\kappa_{el} \to 1$) to the nonadiabatic limit, where $\kappa_{el}\nu_n \propto H_{12}^2$.

IV. NUMERICAL RESULTS

Having outlined reasonably versatile means of formulating the influence of nuclear and electronic quantum corrections on the ET rate both in the presence and absence of solvent friction, it is of interest to examine the combined numerical consequences of such effects, especially regarding their influence upon the anticipated rate-friction dependence in the vicinity of the inertial limit.

Figures 1 and 2 show how the friction influences the magnitude of the nuclear tunneling correction, $\tilde{\Gamma}_n$, as obtained from Eq. (21), with $\omega_o = 5 \times 10^{12}$ or 2.5×10^{13} s^{-1}, respectively, $T = 298$ K, and $\Delta G_c^* = 5.0$ kcal mol^{-1}. The horizontal dashed lines represent the TST limiting values of $\tilde{\Gamma}_n$ for the electronic matrix coupling (H_{12}) values indicated [as given by Eq. (16)], while the corresponding solid curves include the effects of solvent friction. Comparing the $\tilde{\Gamma}_n$ values given in Figs. 1 and 2 illustrates the sensitivity of the nuclear tunneling correction to the magnitude of ω_o as well as to ω_b (i.e. to H_{12}), particularly in the low friction (high τ_L^{-1}) regime. This sensitivity was initially surprising to us. However, the observation becomes readily understandable upon examining the simplest approximate formula for $\tilde{\Gamma}_n$, Eq. (24), in that this relation exhibits an exponential dependence of $\tilde{\Gamma}_n$ upon H_{12}. The inclusion of friction effects, however, reduces the magnitude of $\tilde{\Gamma}_n$ as well as its dependence upon H_{12}.

In a similar fashion, Fig. 3 illustrates how the presence of solvent

friction can diminish the dependence of $\tilde{\Gamma}_n$ upon the reciprocal temperature (K^{-1}) as calculated using Eqs. (16) and (21). The dotted curve representing the nuclear-tunneling correction in the TST limit (for H_{12} = 0.2 kcal mol $^{-1}$) is seen to be significantly more temperature dependent than are the corresponding solid curves which illustrate the influence of friction. The latter show that $\tilde{\Gamma}_n$ decreases markedly with increasing friction; the three solid curves refer to $\tau_L\omega_o$ values of 2, 5, and 20, ω_o being fixed at 2×10^{13} s^{-1}. The dashed curve in the upper left-hand corner of Fig. 3 illustrates further the greater importance of nuclear tunneling for more cusp-like barriers; here H_{12} = 0.05 kcal mol^{-1} with $\tau_L\omega_o$ = 20. The TST results shown in Fig. 3 merit a note of caution, however: Eq. (16) becomes a progressively worse approximation as the temperature approaches the divergence point at $T = \hbar\omega_b/2\pi k_B$. This limitation arises from the presumption that the barrier top can be approximated by an inverted parabola.

Figures 4-7 illustrate how the combination of nuclear and electronic quantum corrections can affect the dependence of the reaction rate on solvent friction, in the form of logarithmic plots of k_{et} versus τ_L^{-1}. (Although we have previously evaluated bimolecular rate constants by spatial integration of k_{et} values so to explore detailed friction-dependent effects[7], attention is restricted here to the latter unimolecular quantity for simplicity). The results in Fig. 4 were calculated by taking H_{12} = 0.2 kcal mol^{-1}, ΔG_c^* = 5.0 kcal mol^{-1}, and T = 298 K (see the Figure Caption for calculational details). The inertial frequency was also fixed at 5×10^{12} s^{-1}; this value was selected as being a typical value for polar solvents (vide supra).[13] The range of τ_L values, 1×10^{11} s^{-1} to 5×10^{12} s^{-1}, reflects that commonly encountered in polar Debye-like media.[6] The solid log k_{et} - log τ_L^{-1} curve was obtained without quantum corrections; the curvature seen towards larger τ_L^{-1} arises entirely from the progressively larger influence of the TST limit set by the chosen inertial frequency. The dotted curve includes the influence

of nuclear tunneling, and the dashed curve the combined effects of nuclear tunneling and electronic nonadiabaticity. (Admittedly, in real experimental systems alterations in τ_L brought about by solvent substitution also yield significant variations in ΔG^* and ω_o. Nevertheless, holding the latter parameters fixed, as in Figs. 4-7, enables their influence on the rate-friction functionality to be more readily discerned).

The accelerating influence of the former quantum effect is seen to be small under these conditions, being swamped by the progressive rate retardation seen towards larger τ_L^{-1} that arises from reaction nonadiabaticity. The latter effect has been discussed in detail recently.[6,7] Not surprisingly, the extent of friction-dependent rate retardation due to reaction nonadiabaticity increases markedly as H_{12} decreases. While the importance of nuclear tunneling also increases under these conditions, reaction nonadiabaticity tends to constitute the dominant quantum effect for a wide range of H_{12} values for the barrier parameters as in Fig. 4.

Significantly different behavior, however, can be obtained under otherwise similar conditions but by choosing somewhat larger ω_o values. This is illustrated in Fig. 5, which contains log k_{et} - log τ_L^{-1} plots obtained as in Fig. 4 but for a fivefold larger ω_o value, 2.5×10^{13} s^{-1}. This inertial frequency is characteristic of relatively small solvent molecules such as acetonitrile (vide supra). Inspection of Fig. 5 shows that while the decelerating effect of reaction adiabaticity still tends to be greater than the accelerating effect of nuclear tunneling (compare solid, dashed curves), the magnitude of the latter is now comparable to the former (compare solid, dotted curves). This is especially the case for high or moderate solvent friction (i.e. lower τ_L^{-1} values).

Given that the numerical importance of nuclear tunneling is sensitive to the temperature (Fig. 3), it is of interest to examine such combined quantum effects on the rate-friction behavior at lower temperatures. For this

purpose, Figs. 6 and 7 contain log k_{et} - log τ_L^{-1} plots calculated as in Figs. 4 and 5, respectively, but with T = 150 K. The markedly enhanced influence of nuclear tunneling is clearly evident in these results. In particular, Fig. 7 (for which $\omega_o = 2.5 \times 10^{13}$ s^{-1}) shows that the rate-decelerating nonadiabatic effects are largely overshadowed by nuclear tunneling, yielding k_{et} values (dashed curve) that are larger than the corresponding classical quantities (solid curve) throughout the range of solvent friction shown.

General Conclusions

One overall conclusion which emerges from such numerical calculations is that the inclusion of such quantum effects can mask partially or even completely the influence of the solvent inertial TST limit on the reaction rate. Electron tunneling rather than nuclear dynamics is often expected to at least partly control the net barrier-crossing velocity [i.e. $\kappa_{el}\nu_n - \nu_{el}$ rather than $\kappa_{el}\nu_n - \nu_n$, Eq. (28)] once the latter approaches the anticipated inertial limit frequencies, ca 10^{13} s^{-1}. Nevertheless, some influence of the inertial dynamics can be anticipated for systems displaying moderate or strong donor-acceptor electronic coupling, say $H_{12} \geq 0.2$ kcal mol^{-1}. While the compensatory influence of nuclear tunneling associated with solvent inertia is typically milder, this factor can mask the rate-limiting effects of both reaction nonadiabaticity and the TST inertial frequency. Given that the quantum effects associated with nuclear tunneling and reaction nonadiabaticity are inherently compensatory and friction-dependent, the common experimental strategy of examining the ET rate-solvent friction dependence[6] may not provide a clear indicator of TST limiting effects. Indeed, the occurrence of the classical solvent-controlled TST limit, whereby the barrier-crossing frequency ($\kappa_{el}\nu_n$) equals $\omega_o/2\pi$, should require the presence of substantial electronic coupling (i.e. large H_{12}) so to both maintain reaction adiabaticity and diminish the importance of nuclear tunneling.

While nuclear tunneling involving solvent inertial motions may often

be small or negligible at room temperature, Fig. 7 illustrates the potential importance of this phenomenon at lower temperatures. Electron-transfer kinetic experiments of this type concerned with solvent dynamical phenomena have apparently yet to be performed. Nevertheless, there are several practical reasons to earmark such studies for future consideration, not the least of which is the markedly diminished reaction rates expected under these conditions.

Quite apart from nuclear tunneling involving solvent rotational/librational modes, substantial quantal effects involving high-frequency reactant vibrational and related solvent modes can often be anticipated. For sufficiently high frequencies (say $\gtrsim 5 \times 10^{13}$ s^{-1}), especially for cusp-like barriers (i.e. small H_{12}), nuclear tunneling involving such modes can be sufficiently important even at ambient temperatures so that their effective contribution to the activation barrier is muted or even essentially removed. Interesting recent calculational examples of such phenomena include $Fe(OH_2)_6^{3+/2+}$ self exchange in aqueous media, for which the presence of substantial nuclear tunneling was deduced for hydrogen atoms motions involving the solvent as well as the aquo ligands.[34] Along with the high ω_o values estimated for water ($\sim 10^{14}$ s^{-1}, vide supra), sizable nuclear-tunneling effects might often be expected in this solvent. Such effects will be lessened substantially, however, for processes featuring strong donor-acceptor orbital overlap, such as the cobaltocenium-cobaltocene self-exchange reaction recently evaluated in water as well as other solvents in our laboratory.[6,35,36] Moreover, the reaction dynamics may well be largely overdamped in water (i.e. solvent friction is prelevant), since $\tau_L^{-1} \ll \omega_o$ (Table I).

The uncertainties in estimating the solvent inertial frequency, noted above, could be construed as providing a major impediment to numerical calculations, especially involving larger and more asymmetric molecules. Fortunately, however, the commonly anticipated prevalence of overdamped motion

for such solvents[18] makes such uncertainties less serious in practice. Of greater anticipated significance is the occurrence of additional *dissipative* relaxations at higher frequencies than τ_L^{-1}. These oft-present components can diminish greatly the effective solvent friction, yielding substantial rate accelerations beyond that anticipated for frequency-independent friction.[9,18,35,36] A quantitative understanding of the influence (or lack thereof) of such high-frequency frictional components, however, will inevitably require detailed consideration of quantum effects.

ACKNOWLEDGMENT

This work is supported by the Office of Naval Research.

Epilogue

Dr. George McManis died tragically in October 1989, just prior to our receiving the invitation to submit this article. The selection of material in the present manuscript was determined in part by George's central role in its conception, evolution, and communication. We are most pleased to publish it in his memory (AG, MJW).

Appendix A: Derivation of Eq. (2) and Related Considerations

Equation (2) can be generalized to include a somewhat more involved definition of ω_f than Eq. (2a). The free rotor frequency, ω_f, is defined as:[9,37]

$$\omega_f^2 = \langle\omega\cdot\omega\rangle - \langle(u\cdot\omega)^2\rangle = \langle\dot{u}^2\rangle \qquad A.1$$

where ω is the molecular angular velocity vector, and u is the unit vector that lies along molecular dipole moment vector, μ. Here, we will explore the derivation more fully, following Hynes[9] and Brot.[37] Evaluating $\omega_f^2 = \langle\omega\cdot\omega\rangle - \langle(u\cdot\omega)^2\rangle$ term by term, we find

$$\omega_f^2 = \langle\omega_x^2 + \omega_y^2 + \omega_z^2 - (u_x\omega_x + u_y\cdot\omega_y + u_z\cdot\omega_z)^2\rangle \qquad A.2$$

Evaluating the square, and taking advantage of the fact that cross terms in Eq. (A.2) vanish, allows the simplification:[37]

$$\omega_f^2 = \langle\omega_x^2 + \omega_y^2 + \omega_z^2 - [(u_z^2 + u_y^2)\omega_x^2 + (u_y^2 + u_x^2)\omega_z^2 + (u_z^2 + u_x^2)\omega_y^2]\rangle \qquad A.3$$

Since u is a unit vector, $u_x^2 + u_y^2 + u_z^2 = 1$, where u_x, u_y and u_z are the projections of the unit vector along the dipole moment onto the principal axes of inertia, the formula for ω_f^2 in equation A.3 (after inserting the equipartition values for ω, i.e. $\omega_\alpha^2 = k_BT/I_\alpha$) becomes:[37]

$$\omega_f^2 = k_BT\left[\frac{(u_x^2 + u_y^2)}{I_z} + \frac{(u_y^2 + u_z^2)}{I_x} + \frac{(u_x^2 + u_z^2)}{I_y}\right] \qquad A.4$$

or, restated in more compact form,

$$\omega_f^2 = k_BT\sum_\alpha\left(\frac{\mu^2 - \mu_\alpha^2}{\mu^2}\right)(I_\alpha^{-1}) \qquad A.5$$

where $\mu^2 = \mu^T\mu$ (T connotes the vector transpose)and $\alpha = x,y,z$ This more general expression reduces to Eq. (2a) in the text for linear and spherical-top molecules.

The three individual components of the complete dipole moment vector can be derived from the Stark effect splitting of the [gas phase] rotational spectra for the molecule. (Dipole moments are often markedly different in condensed phase than in vacuum[38] so the use of these parameters generates some uncertainty in estimating ω_o.) The principal moments of inertia may be extracted from tabulations of the three rotational constants, R_α (usually called A, B and C, respectively), using the relation:[37]

$$R_\alpha = \frac{\hbar}{4I_\alpha c} \qquad \text{A.6}$$

where c is the speed of light.

The dielectric parameter terms in Eq. (2) arise from the form of the dielectric response function, expressed as the dielectric permittivity $\hat{E}(s)$:[37,39]

$$\hat{E}(s) = \left(1+ \frac{3\epsilon_s}{2\epsilon_s + \epsilon_\infty} \left[\frac{g_k}{\mathcal{L}(-\dot{g}(t))} - 1\right]\right)^{-1}$$

$$= \frac{\hat{\epsilon}(s) - \epsilon_\infty}{\epsilon_s - \epsilon_\infty} = \frac{2\epsilon_s + \hat{\epsilon}(s)}{3\epsilon_s g_k} \mathcal{L}(-\dot{g}(t)) \qquad \text{A.7}$$

where $\dot{g}(t) = \partial g(t)/\partial t$. Equation A.7 utilizes the notion of the time-dependent Kirkwood "g" factor - a collective function describing the structural correlations in the ensemble of solvent molecules. If the structural-correlation function decays exponentially in time, $\mathcal{L}(-\dot{g}(t)) \propto 1/(1 + s\tau^*)$, in which case $\hat{E}$ becomes a simple exponential with the relaxation time, τ^*, characterizing the decay of the structural correlation function g(t); τ^* is related to the Debye relaxation time τ_D by:[37,39]

$$\tau_D = \frac{3\epsilon_s}{2\epsilon_s + \epsilon_\infty} \tau^* \qquad \text{A.8}$$

As pointed out by Hynes, g(t) obeys a Langevin equation having the usual

form:[9]

$$\dot{g}(t) = -\int_0^t d\tau\ K(t - \tau)\ g(\tau) \qquad A.9$$

where the kernel, K(t), has the Laplace transform:

$$\tilde{K}(s) = \frac{\tilde{K}(0)}{s + \xi_L(s)} = \frac{\omega_f^2}{g_K[(s + \xi_L(s)]} \qquad A.10$$

The frictional term $\xi_L(s)$ contains the dielectric loss information. The kernel, $\tilde{K}(0)$ in Eq. (A.10), equals ω_f^2/g_k.[9] Inserting this into the overall expression for the dielectric response function $\hat{E}(s)$ as given in equation A.7, the high frequency term (multiplied by s^2) can be identified as an "inertial limited" transverse frequency if we assume a friction coefficient having the form $\xi_T(s) = \omega_T^2\ \tau_D(s)$.[37] Assuming $\tau_D(s) = \tau_D$ (i.e. Debye behavior), $\hat{E}(s)$ can then be reexpressed as:

$$\hat{E}(s) = \{1 + \frac{s^2}{\omega_T^2} + s\tau_D\}^{-1} \qquad A.11$$

where ω_T is now identified as:

$$\omega_T^2 = \frac{2\epsilon_s + \epsilon_\infty}{3\epsilon_s}\ \frac{\omega_f^2}{g_k} \qquad A.11a$$

One then extracts the corresponding longitudinal quantity, ω_o, using [cf Eq. (9)]:[40]

$$\omega_o = \omega_T\ (\epsilon_s/\epsilon_\infty)^{1/2} \qquad A.12$$

which yields

$$\omega_o^2 = \frac{(2\epsilon_s + \epsilon_\infty)\ \omega_f^2}{3\epsilon_\infty\ g_k} \qquad A.13$$

Eq. (A.13) is identical with Eq. (2) in the text. It is also worth noting that the proportionality coefficient relating the transverse and longitudinal inertial frequencies ω_T and ω_o in Eq. (A.12), $(\epsilon_s/\epsilon_\infty)^{1/2}$, is similar to but not identical with the well-known factor $(\epsilon_s/\epsilon_\infty)$ relating the transverse and longitudinal *overdamped* relaxation frequencies τ_D^{-1} and τ_L^{-1}. A detailed

derivation of Eq. (A.12) along with a discussion of the underlying physics responsible for these differences is to be found in Appendix A of ref. 30.

Appendix B: A Numerical Comparison of Nuclear-Tunneling Corrections

We outlined above a number of different approximate formulations of the nuclear tunneling correction factor Γ_n. Table B.I presents a numerical comparison of Γ_n values using Eqs. (16), (17), and (24) for three different values of H_{if} and ω_o. It is seen that all three expressions yield similar results when $\omega_o = 5 \times 10^{12}$ s^{-1}. However, significant discrepancies (even divergences!) are obtained at larger values of ω_o, particularly for small values of H_{12}.

Table B.I

A Comparison of Nuclear Tunneling Correction Factors in the Transition State Theory Limit at 298 K

Approximation	H_{12} [a] (kcal mol^{-1})	Γ_n [b] $\omega_o = 5\times10^{12}$ (s^{-1})	$\omega_o = 1\times10^{13}$ (s^{-1})	$\omega_o = 2.5\times10^{13}$ (s^{-1})
Equation 16	0.05	1.15	1.87	[c]
	0.125	1.06	1.34	10.04
	0.2	1.04	1.26	2.92
Equation 17	0.05	1.15	1.86	[c]
	0.125	1.06	1.33	9.87
	0.2	1.03	1.25	2.87
Equation 24	0.05	1.15	1.79	5.41
	0.125	1.06	1.32	3.93
	0.2	1.04	1.25	2.35

[a] The cusp barrier height was taken as $\Delta G_c^* = 5.0$ kcal mol^{-1}.

[b] The barrier top frequency, ω_b, was calculated using Eq. (10).

[c] No numerical estimate could be obtained owing either to divergence in the expression or violation of boundary conditions for the approximation.

REFERENCES

1. M. J. Weaver, G. E. McManis, Acc. Chem. Res., 23 (1990), 294.

2. M. Maroncelli, J. MacInnis, G. R. Fleming, Science, 243 (1989), 1674; G. R. Fleming, P. G. Wolynes, Physics Today, May 1990, p. 36.

3. P. F. Barbara, W. Jarzeba, Adv. Photochem., 15 (1990), 1.

4. G. van der Zwan, J. T. Hynes, J. Phys. Chem., 89 (1985), 4181.

5. D. F. Calef, P. G. Wolynes, J. Phys. Chem., 87 (1983), 3387.

6. G. E. McManis, R. M. Nielson, A. Gochev, M. J. Weaver, J. Am. Chem. Soc., 111 (1989), 5533.

7. A. Gochev, G. E. McManis, M. J. Weaver, J. Chem. Phys., 91 (1989), 906.

8. For example, see: M. D. Newton, N. Sutin, Ann. Rev. Phys. Chem., 35 (1984), 437.

9. J. T. Hynes, J. Phys. Chem., 90 (1986), 3701.

10. See for example, G. Wyllie, "Dielectric and Related Molecular Processes", Vol. I, The Chemical Society, London, 1972, Ch. 2; C. Brot, ibid, Volume II, 1975, Ch. 1.

11. See for example: H. L. Friedman, "A Course in Statistical Mechanics", Prentice-Hall, Englewood Cliffs, NJ, 1985, Ch. 8.

12. S. A. Adelman, J. M. Deutch, Adv. Chem. Phys., 31 (1975), 103.

13. P. Madden, D. Kivelson, Adv. Chem. Phys., 56 (1984), 467.

14. J. Ph Poley, App. Sci. Res., B4 (1955), 337.

15. For example, see: (a) B. J. Bulkin, Helv. Chim. Acta, 52 (1969), 1349; (b) C. J. Reid, J. K. Vij, P. L. Rosselli, M. W. Evans, J. Mol. Liq., 29 (1984), 37; (c) N. Hill, Proc. Phys. Cog., 78 (1961), 311; (d) Y. Leroy, E. Constant, C. R. Hebd, Science Acad. Sci., 262 (1966), 1391.

16. M. Evans, G. J. Evans, W. T. Coffey, P. Grigolini, "Molecular Dynamics and Theory of Broad Band Spectroscopy", John Wiley and Sons, New York (1982), Ch. III, IV.

17. S. Lee, J. T. Hynes, J. Chem. Phys., 88 (1988), 6863.

18. G. E. McManis, M. J. Weaver, J. Chem. Phys., 90 (1989), 912.

19. (a) M. Neumann, J. Chem. Phys., 82, 5663 (1985). (b) M. Neumann, J.

Chem. Phys., 85 (1986), 1567.

20. D. M. F. Edwards, P. A. Madden, I. R. McDonald, Mol. Phys., 51 (1984), 1141.

21. J. McConnell, "Rotational Brownian Motion and Dielectric Theory", Academic Press, London (1980), Chap. 11.

22. J. T. Hynes, in "The Theory of Chemical Reaction Dynamics", M. Baer, ed., CRC Press, Boca Raton, FL, Vol. 4, 1985, Ch.4.

23. R. F. Grote, J. T. Hynes, J. Chem. Phys., 73 (1980), 2715.

24. P. Hanggi, J. Stat. Phys., 42 (1986), 105.

25. (a) Yu. I. Daknovskii, A. Ovchinnikov, Mol. Phys., 58 (1986), 237; (b) Yu. I. Daknovskii, A. Ovchinnikov, Phys. Lett., 113A (1985), 147; (c) Yu. I. Daknovskii, A. Ovchinnikov, Khim. Fiz., 5 (1986), 36.

26. (a) S. G. Christov, Ber. Bunsenges. Phys. Chem., 76 (1972), 507; (b) S. G. Christov, Ber. Bunsenges. Phys. Chem., 78 (1974), 537; (c) S. G. Christov, Ber. Bunsenges. Phys. Chem., 79 (1975), 357; (d) S. G. Christov, "Collision Theory and Statistical Theory of Chemical Reactions", Lecture Notes in Chemistry, Vol. XVIII, Springer-Verlag, Berlin (1980).

27. S. G. Christov, Int. J. Quant. Chem., 36 (1989), 391.

28. (a) T. Holstein, Ann. Phys., (N.Y.), 8 (1959), 325; (b) T. Holstein, Ann. Phys., (N.Y.), 8 (1959), 343; (c) T. Holstein, Phil. Mag., 37 (1978) 49; (d) T. Holstein, Phil. Mag., 37 (1978), 499.

29. P. G. Wolynes, Phys. Rev. Lett., 47 (1981), 968.

30. G. E. McManis, Ph.D. dissertation, Purdue University, 1989.

31. (a) E. Wigner, Z. Phys. Chem., B19 (1932), 203; (b) J. O. Hirschfelder, E. Wigner, J. Chem. Phys., 7 (1939), 616.

32. G. E. McManis, A. K. Mishra, M. J. Weaver, J. Chem. Phys., 86 (1987), 5550.

33. (a) D. N. Beretan, J. N. Onuchic, J. Chem. Phys., in press; (b) J. N. Onuchic, D. N. Beretan, J. Phys. Chem., 92 (1988), 4818.

34. J. S. Bader, R. Kuharski, D. Chandler, J. Chem. Phys., in press.

35. R. M. Nielson, G. E. McManis, M. J. Weaver, J. Phys. Chem., 93 (1989), 4703.

36. M. J. Weaver, G. E. McManis, W. Jarzeba, P. F. Barbara, J. Phys. Chem., 94 (1990), 1715.

37. C. Brot, in "Dielectric and Related Molecular Processes", Volume II, The Chemical Society, London (1975), p. 1.

38. For numerous examples, see: A. L. McClellan, "Tables of Experimental Dipole Moments", W. H. Freeman Co., San Francisco, (1963).

39. C. J. F. Bottcher, O. C. Van Belle, P. Bordewijk, A. Rips, "Theory of Electric Polarization", Vol. I, Elsevier, Amsterdam, 1973, Ch. VI.

40. H. Frolich, "Theory of Dielectrics", Oxford University Press, 1958, Chapter IV.

TABLE I Comparison Between Inertial Frequencies Estimated from Eq. (2) and Inverse Longitudinal Relaxation Times for Some Common Solvents at 25°C.

Solvent	τ_L^{-1} [a] ps^{-1}	ω_o [b] ps^{-1}
Acetonitrile	4	11
D_2O	1.9	40
Dimethylsulfoxide	0.5	9.5
Benzonitrile	0.2	4
Hexamethylphosphoramide	0.11	~4
Methanol	(0.135)	11
Ethanol	(0.033)	9.5

[a] Inverse longitudinal relaxation times for solvent indicated, as obtained from dielectric loss data (see ref. 6 for data sources). Values for methanol and ethanol (given in parentheses) refer to large-amplitude, longer time, portion of multicomponent dielectric disposition.

[b] Solvent inertial frequency, estimated from Eq. (2) (see ref. 18 for data sources).

FIGURE CAPTIONS

Fig. 1

Nuclear-tunneling correction to rate constant as a function of log τ_L^{-1}, where τ_L is the solvent longitudinal relaxation time, for three different electronic matrix coupling elements H_{12} as indicated, calculated from Eqs. (10) and (21). The dashed horizontal lines represent the TST limiting value (i.e. for $\tau_L \to 0$), calculated from Eqs. (10) and (16). Other parameters: $\omega_o = 5 \times 10^{12}$ s^{-1}, $\Delta G_c^* = 5.0$ kcal mol^{-1}, T = 298 K.

Fig. 2

As in Fig. 1, but for H_{12} values indicated with a higher inertial limiting frequency, $\omega_o = 2.5 \times 10^{13}$ s^{-1}.

Fig. 3

Nuclear-tunneling correction factors as a function of the reciprocal absolute temperature. Solid curves refer to τ_L values (in order of decreasing $\tilde{\Gamma}_n$) equal to $2/\omega_o$, $5/\omega_o$, and $20/\omega_o$, with $H_{12} = 0.2$ kcal mol^{-1}, calculated by using Eqs. (10) and (21). Dashed curve refers to $\tau_L = 20/\omega_o$ and $H_{12} = 0.05$ kcal mol^{-1}. Dotted curve represents the TST result (i.e. for $\tau_L \to 0$) for $H_{12} = 0.2$ kcal mol^{-1} obtained from Eqs. (10) and (16). Other parameters: $\omega_o = 2 \times 10^{13}$ s^{-1}, $\Delta G_c^* = 5.0$ kcal mol^{-1}.

Fig. 4

Logarithmic plot of the unimolecular ET rate constant, k_{et}, versus the inverse longitudinal solvent relaxation time. Solid curve is the classical adiabatic result, obtained from Eqs. (1), (10)-(13), and (15), with $\omega_o = 5 \times 10^{12}$ s^{-1}, $H_{12} = 0.2$ kcal mol^{-1}, $\Delta G_c^* = 5.0$ kcal mol^{-1}, T = 298 K. Dotted curve includes nuclear tunneling correction as calculated from Eq. (21). Dashed curve includes additionally the electronic transmission coefficient (i.e. reaction nonadiabaticity) calculated from Eq. (28).

Fig. 5

As in Fig. 4, but for $\omega_o = 2.5 \times 10^{13}$ s^{-1}.

Fig. 6

As in Fig. 4, but for T = 150 K.

Fig. 7

As in Fig. 4, but for $\omega_o = 2.5 \times 10^{13}$ s^{-1} and T = 150 K.

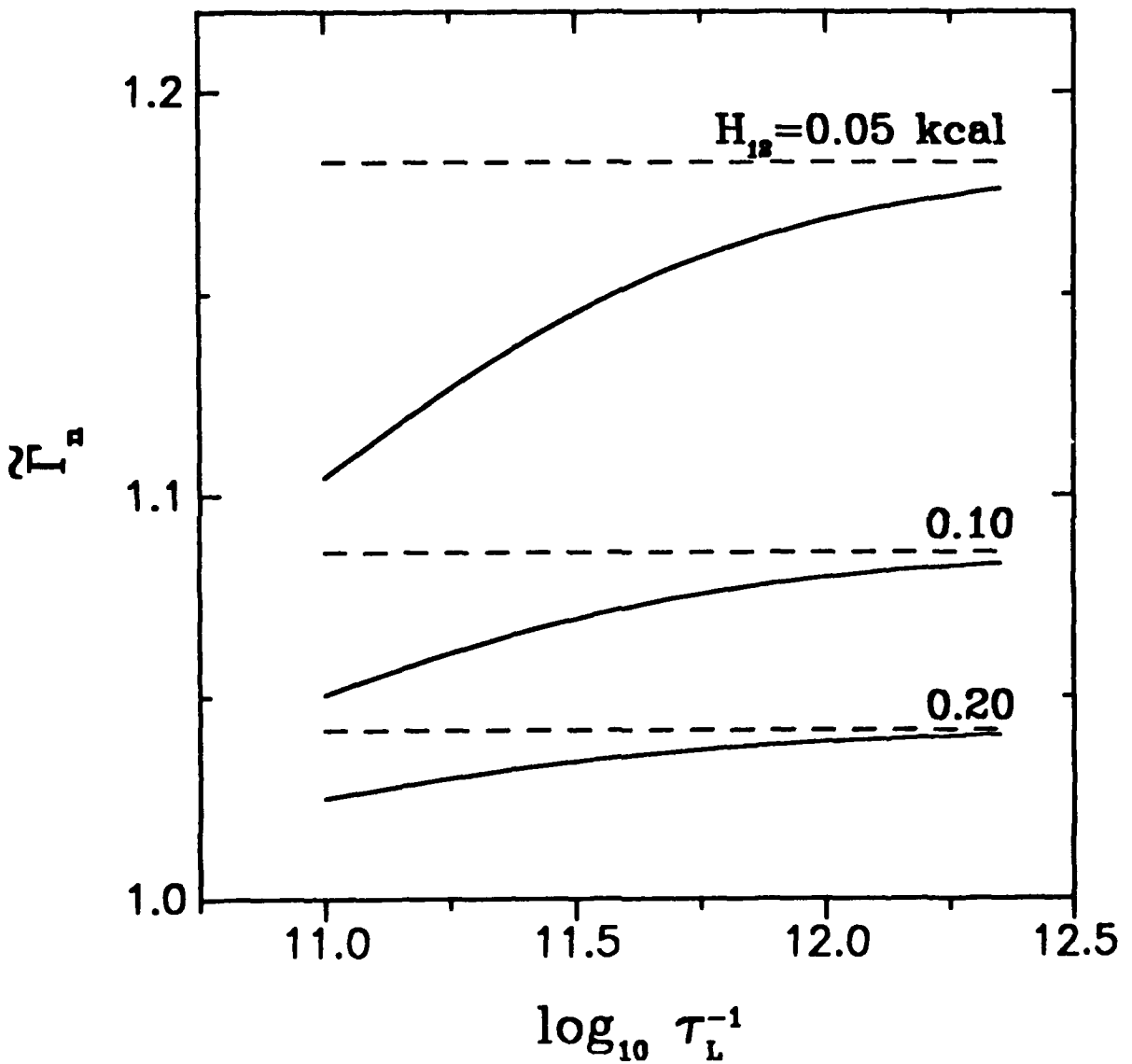

FIG 1

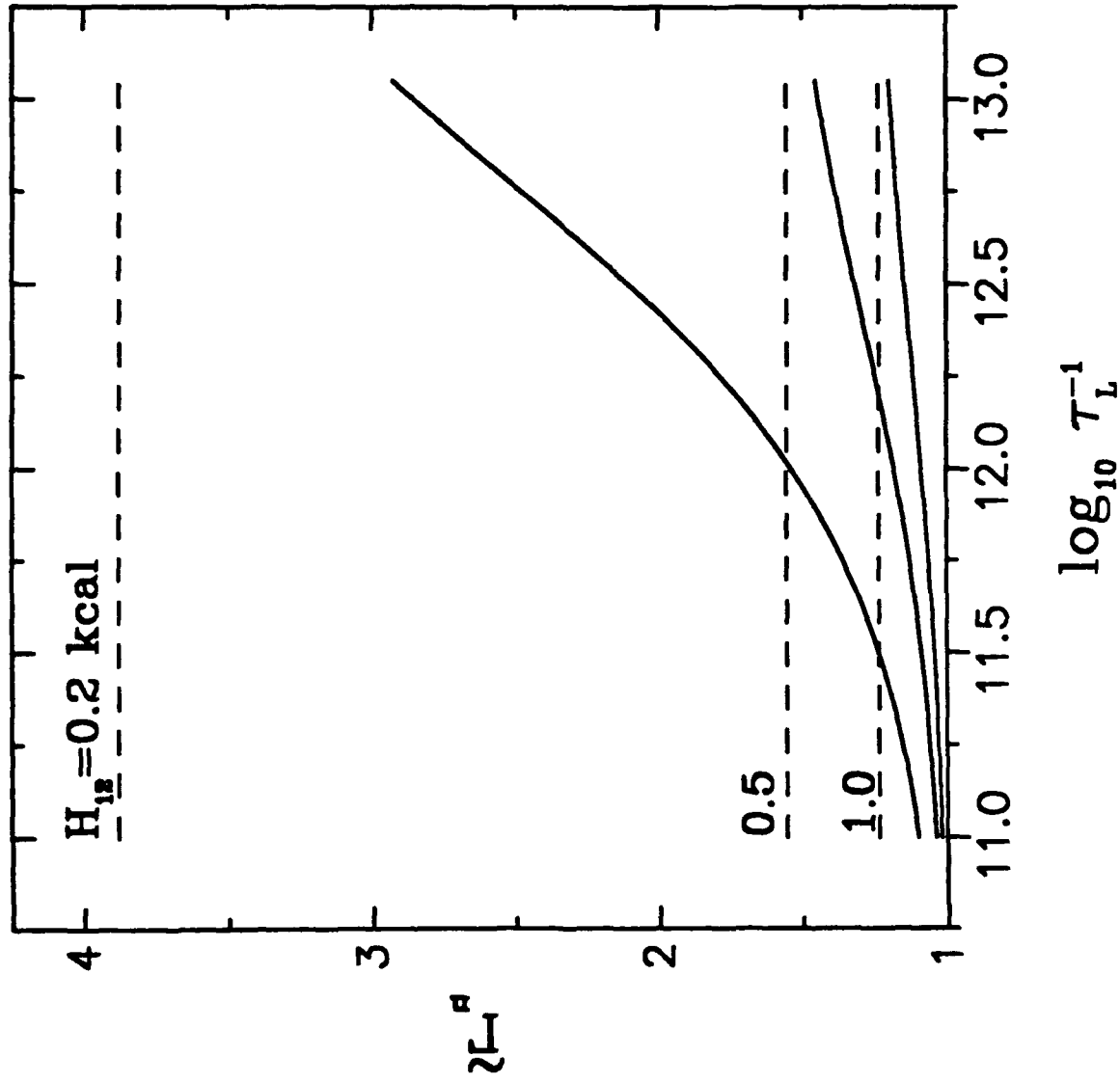
H_{12}=0.2 kcal
0.5
1.0
4
3
2
1
11.0
11.5
12.0
12.5
13.0
$\log_{10} \tau_L^{-1}$
$2\Gamma_1^a$

FIG 2

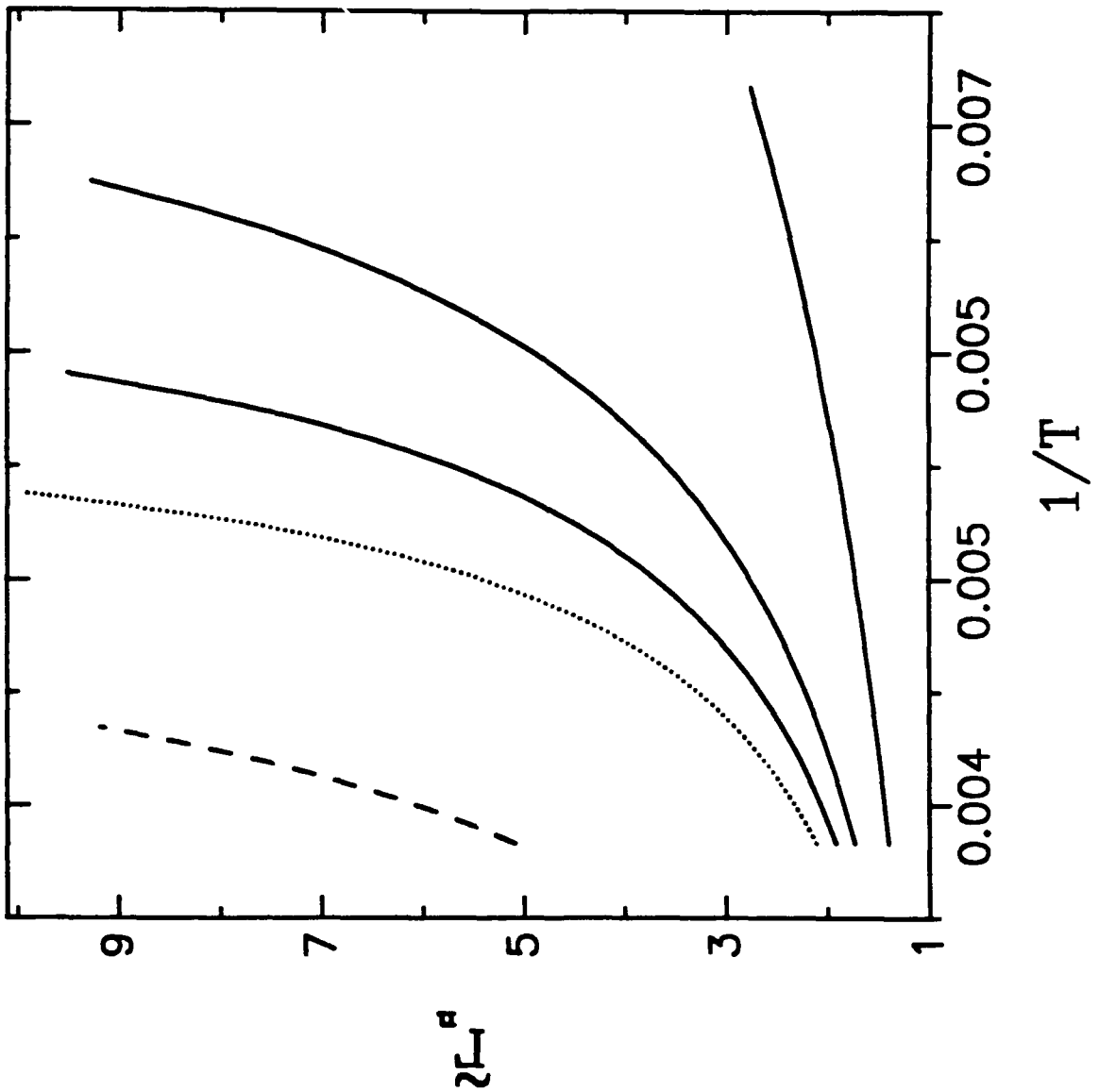

FIG 3

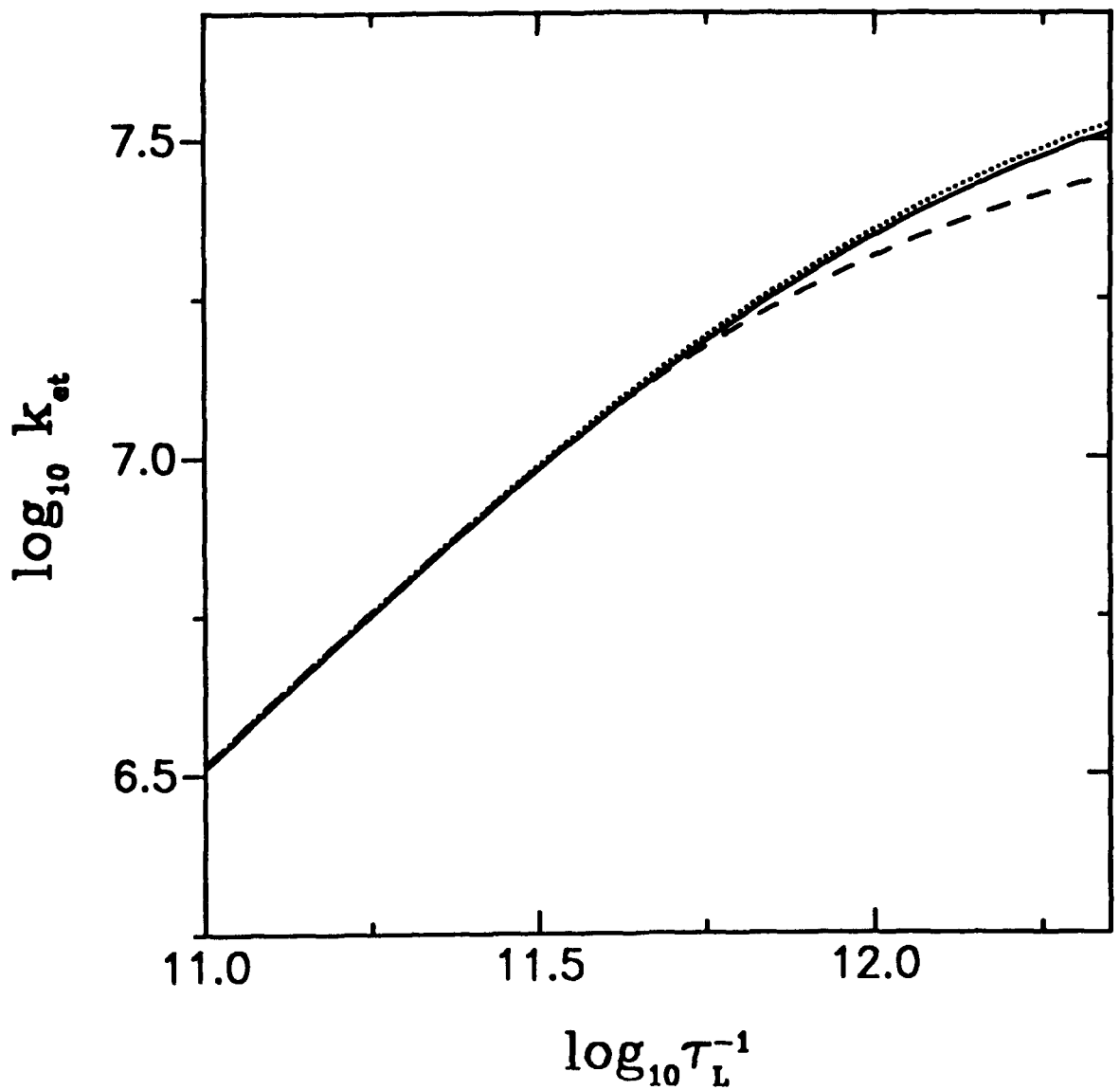

Fig 4

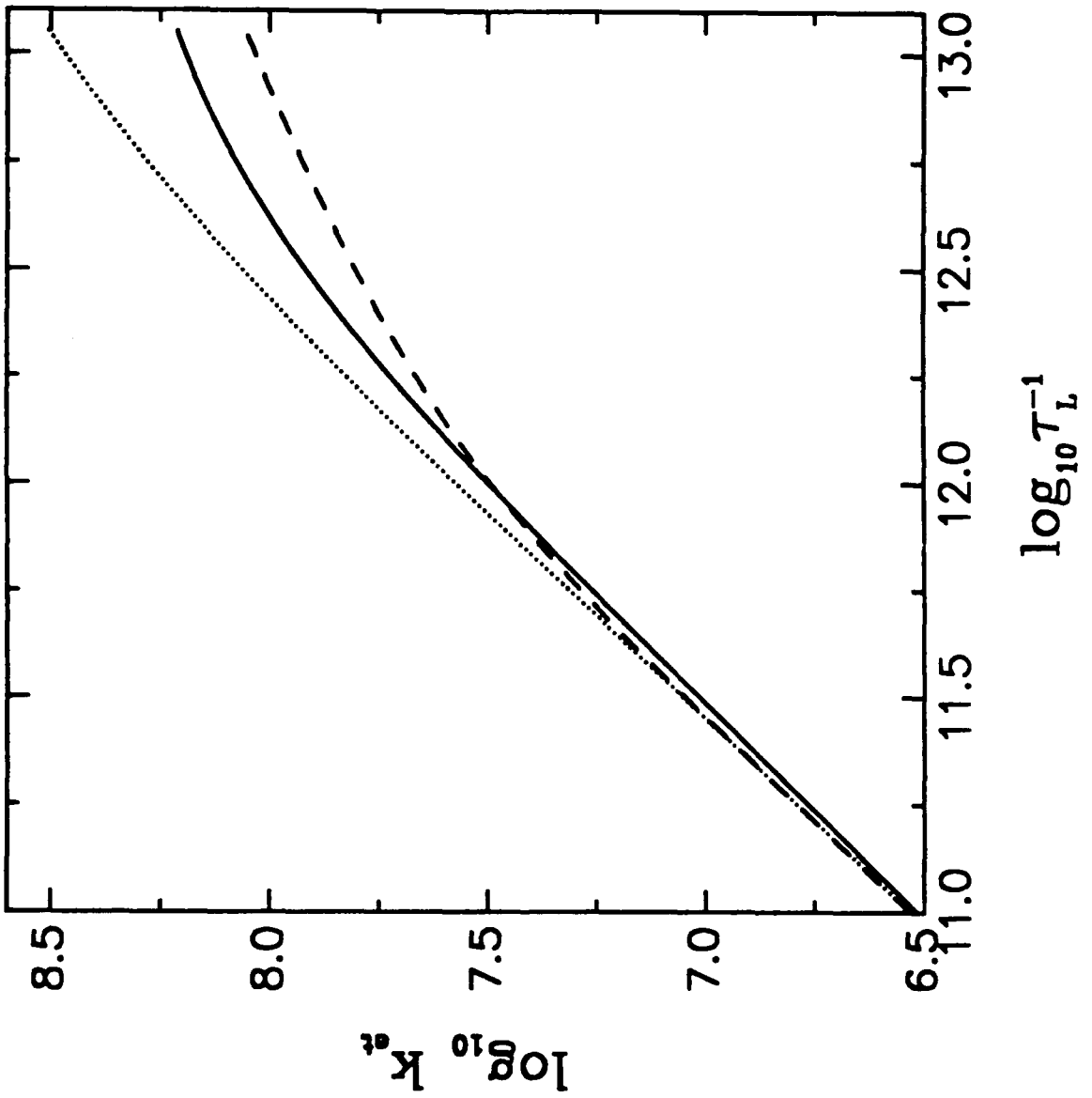

FIG 5

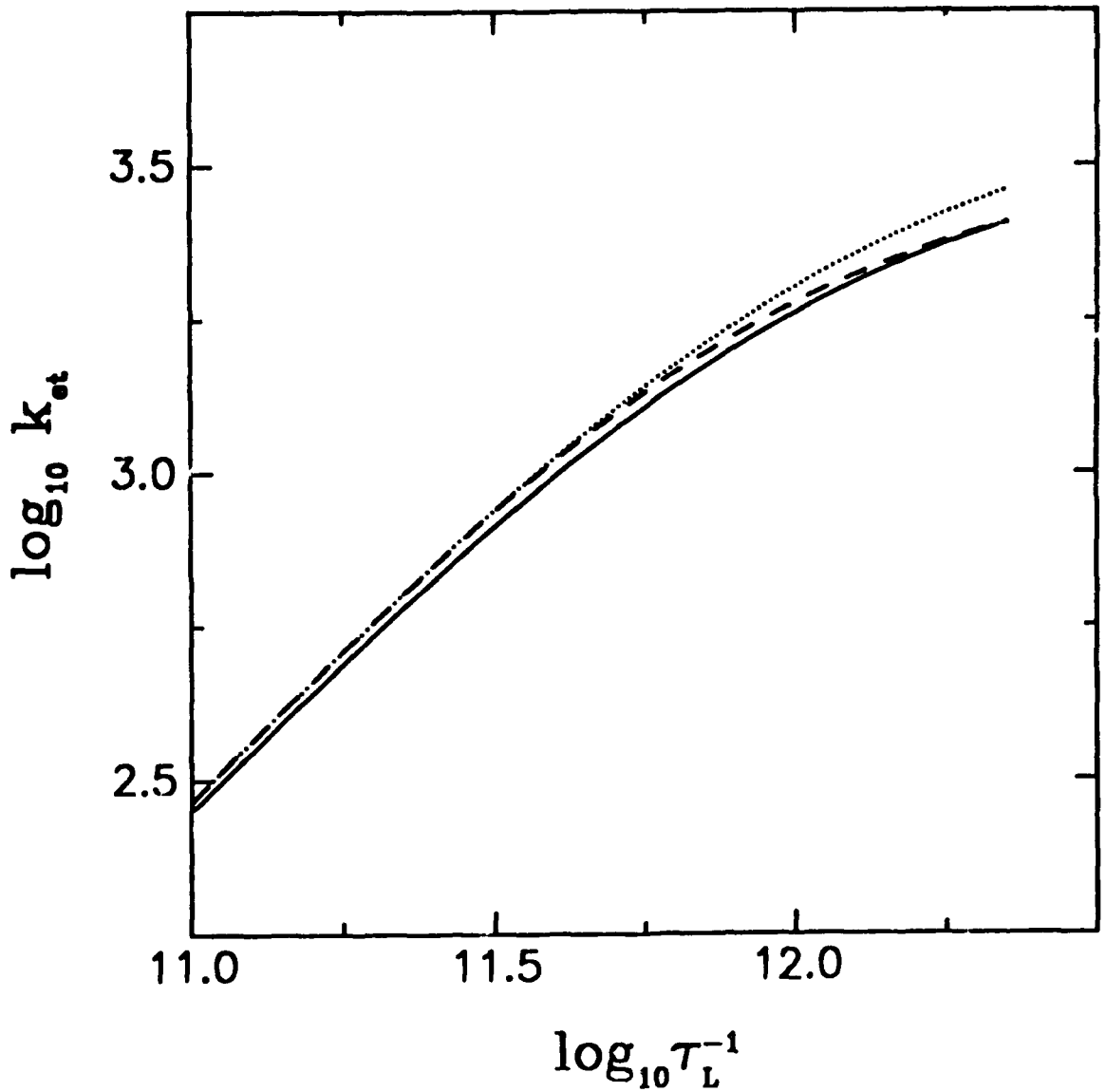

Fig. 6

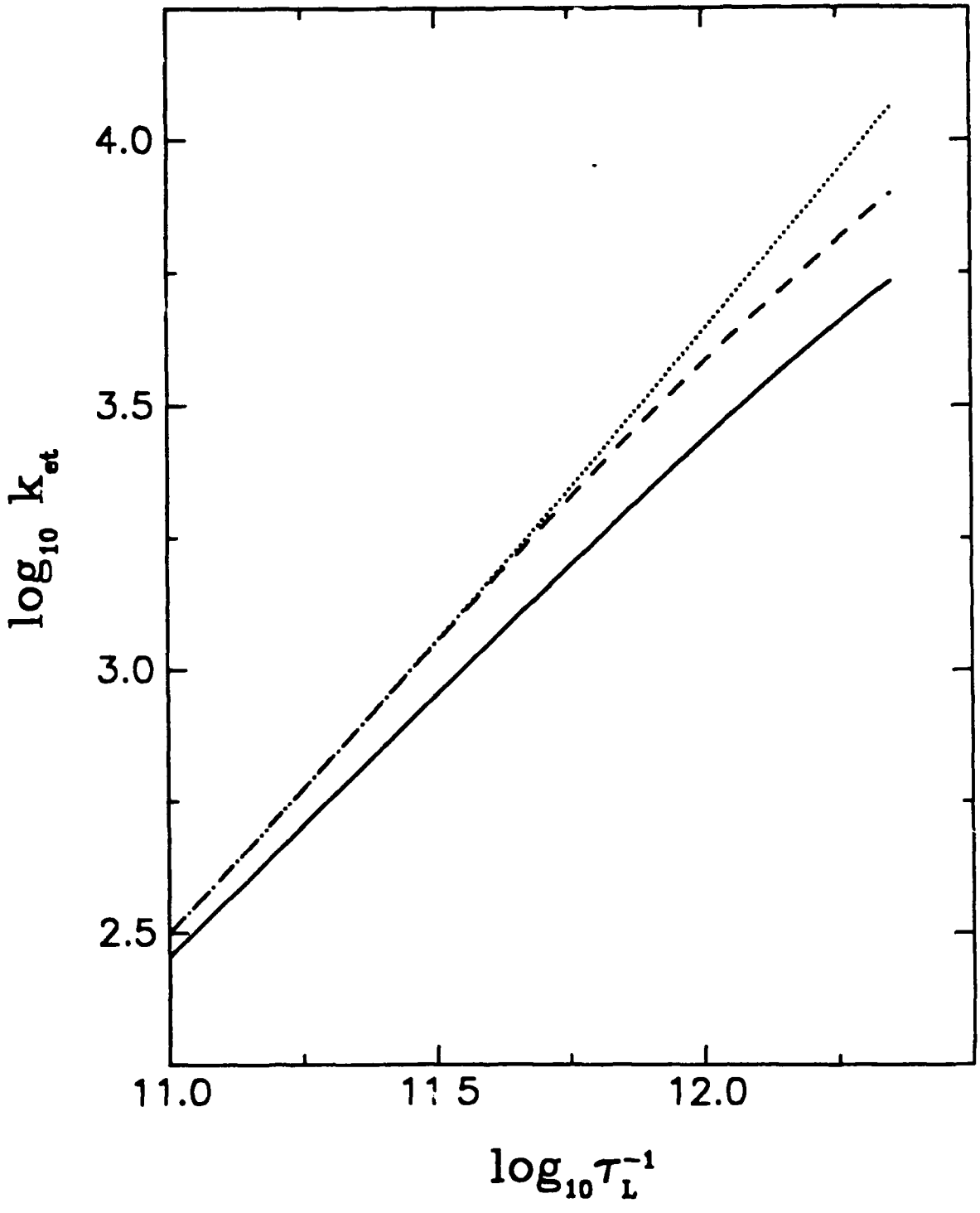

FIG 7